www.vbripress.com/aml, DOI: 10.5185/amlett.2016.6050 Published online by the VBRI Press in 2016

Nanocrystalline diamond films as a protective coating for implantable bio- devices

Rishi Sharma[1], Neelima Sharma[2]*, Rahul Parmar[1], Vijay Chatterjee[1], Anoop Kumar[2], N. Woehrl[3], V. Buck[3], P. K. Barhai[1]

[1]*Plasma Thin Film Laboratory, Department of Physics, Birla Institute of Technology, Mesra 835215, Ranchi, India*
[2]*Department of Pharmaceutical Sciences and Technology, Birla Institute of Technology, Mesra 835215, Ranchi, India*
[3]*Division of Thin Film Technology, Faculty of Physics, University of Duisburg-Essen, 47048 Duisburg and CeNIDE, Germany*

*Corresponding author. Tel: (+91) 651-2275444/2275896; E-mail: neelimarsharma@hotmail.com

Received: 02 July 2015, Revised: 22 February 2016 and Accepted: 22 May 2016

ABSTRACT

Nanocrystalline diamond (NCD) films are deposited on silicon substrates using Microwave Plasma Enhanced Chemical Vapor Deposition technique with the variation of microwave power from 800 W to 1800 W at 200 mbar for 5 hrs. Methane is used as a precursor along with argon and hydrogen as carriers for deposition. Deposited films are characterized by using Raman, FTIR, optical contact angle, AFM and SEM. The biocompatibility study has been carried out by cell viability assay, haemolysis test and simulated body fluid (SBF) adsorption assay. The Lymphocytes and Fibroblast cell lines are cultured on the NCD coated samples and cell viability has been determined by MTT assay. The surface morphology of the samples has been studied by using AFM, before and after interaction with SBF. It has been observed that NCD coated substrates are biocompatible, haemocompatible and also promote the growth of the cells, while the uncoated substrates cause cell death. Copyright © 2016 VBRI Press.

Keywords: Nanocrystalline diamond films; lymphocytes; fibroblast cell lines; simulated body fluid; haemocompatibility.

Introduction

Nanostructured materials are becoming increasingly important in the development of biomedical devices and implants. A large number of artificial medical devices such as hip joints, heart valves, dental roots, intraocular lenses etc. are implanted into the human body every day [**1**]. Current implantable biomaterials such as Ti alloys and ultrahigh molecular weight polyethylene, Poly(methyl methacrylate) face many problems such as degradation, wear and corrosion, which result the shortening of service time. The degradation of biomaterials can also result in reactions and infection of the sensitive tissues with the prostheses [**2**]. It is the surface of the biomaterials, which directly comes in contact with living tissues and body fluid when the implants are placed inside the body. Living organism, cells, tissues and blood interact with the surface of implanted biomaterial and respond according to the surface properties. Therefore, it is necessary that implant's surface should be biocompatible and should not have any toxic effect. However, very few surfaces are truly biocompatible.

It is difficult to fabricate whole device or implants with biocompatible materials but the surface of the implants or device can be modified by the coating of biocompatible materials. Diamond which is known to its superlative mechanical properties like hardness, low wear and chemical inertness can be considered as true biocompatible material [**3**]. But the well-known fact is that the diamond as a bulk can neither be used for implants nor for coatings. Modern techniques like Microwave-PECVD, RF-PECVD, DC-PECVD, sputtering etc., provide an alternative of bulk diamond in the form of carbon thin films like Diamond like Carbon films, Nanocrystalline diamond films, Microcrystalline diamond films etc. [**3-6**]. These films possess many beneficial mechanical and chemical properties sometimes superior to that of diamond. These films can be coated on substrates of any shape and size. Diamond-like carbon coatings is the preferred choice for coating as a biocompatible material [**7-13**]. However, internal stress, low thickness and poor adhesion limit its applicability [**4, 14, 15**].

Nanocrystalline diamond (NCD) films which possess numerous valuable physical, chemical and mechanical properties can be explored as biocompatible materials [5]. Biocompatibility study of NCD films as substrate/scaffold materials for bioengineering have not been performed to meaningful extent. However, research on biocompatible materials is going on but the true biocompatible materials are yet to be discovered [**16, 17**].

When a device is implanted in the body it interacts with blood, muscles and body fluids. NCD coating of implanted devices may improve the performance and lifetime, as well as their biocompatibility. This work aims to evaluate the cytotoxicity profile and biocompatibility of NCD-coated silicon samples, regarding the use of this material combination in biomedical applications. Hence, in the present investigation, the interaction of uncoated silicon and NCD coated silicon with lymphocyte cells, fibroblast cell lines, simulated body fluid (SBF) and blood has been accessed. Prior to biocompatibility test deposited films are also characterized using Raman, FTIR, optical contact angle, AFM and SEM. Effect of the interaction of SBF with the samples has been analyzed by using AFM.

Experimental

Deposition of NCD films

Six NCD films are deposited in a CYRANNUS® I – 6" microwave plasma enhanced chemical vapour deposition (microwave-PECVD) system (Make: iplas GmbH, Germany) using a mixture of $Ar/H_2/CH_4$ (purity 99.999%) on Si wafer (both side polished n-type <100>). Deposition is carried out at constant pressure (200 mbar), constant temperature (600°C) and fixed gas composition (96.7 % Ar, 0.8 % CH_4, 2.5 % H_2; total flow 400 sccm), with the variation of microwave power from 800 to 1800 Watt for 5 hours. Silicon substrates (size 10×10 mm^2) are placed on a molybdenum substrate holder which is placed on a stainless steel stage. During deposition, the microwave plasma ball is adjusted in such a way that the substrates remain in direct contact with the microwave discharge. The substrate temperature is measured by an optical pyrometer. Discharge uniformity, substrate temperature uniformity and hence, deposition uniformity are achieved over the substrate diameter by careful adjustment of the cavity tuning. In this deposition configuration, the substrate holder and the substrate are not heated by external heat source and thus, all the energy supplied to the substrate is supplied by the microwave discharge. Variable cooling arrangement by using a custom designed aerosol cooling is attached with the substrate stage, therefore, the substrate temperature is kept constant (600 °C) throughout the process. The deposition parameters of NCD films are shown in **Table 1**. Prior to deposition, the substrates are pre-treated with mechanical scratching with diamond powder (0.1 µm size) followed by an ultrasonic bath cleaning with acetone and etched with H_2/Ar plasma for 30 min.

Table 1. Deposition parameters of NCD films.

S. No.	Name of the sample	Microwave power (watt)	Deposition Time (hours)	Pressure (m bar)
1	NCD 1	800	5	200
2	NCD 2	1000	5	200
3	NCD 3	1200	5	200
4	NCD 4	1400	5	200
5	NCD 5	1600	5	200
6	NCD 6	1800	5	200

Characterization of NCD films

The deposited films are characterized using Raman spectroscopy (in Via Reflex Raman Spectrometer, Renishaw, U.K.), Fourier transform infrared (FTIR) spectroscopy (SHIMADZU IR prestige-21, Japan), scanning electron microscopy (SEM) (JEOL JSM 6390LV, USA), atomic force microscopy (AFM) (NT-MDT Solver pro 47 AFM, USA) and contact angle setup (Data Physics, Germany). FTIR spectra are recorded in Attenuated Total Reflectance mode at ambient temperature and pressure. SEM measurements are carried out at 10 kV. AFM is used in lateral force (LF) mode. LF mode is useful for imaging variations in surface friction that can arise from in homogeneity in surface material and also for obtaining edge-enhanced image of any surface.

Biocompatibility studies of NCD films

Cell viability assay in lymphocytes

Lymphocytes are collected from albino mice and single cell suspension is prepared under aseptic conditions. The suspension is filtered through 100micron filter and centrifuged at 3000 rpm for 10 min at 4ºC. Lymphocytes are re-suspended in RPMI-1640 medium [**18**]. The cells are seeded on the substrates at a density of 1.0×10^4 cells in a 96-well plate and incubated for 72 h at 37^0C in a CO_2 incubator. Ten microlitres (µl) of 3(4,5-dimethyl-2-yl)-2,5-diphenyl tetrazolium bromide (MTT), 5mg/ml in Phosphate buffered saline is added to the wells, 4 h prior to the completion of incubation time. The plate is centrifuged at 1200×g for 10 min and 100 µl of dimethyl sulfoxide (DMSO) is added after removing the supernatant, to dissolve the formazan formed. The absorbance is read at 530 nm after 5 min, in a microplate reader (Synergy HT of BIO-TEK International, USA) [**19**].

Cell viability assay in fibroblast cell line (NIH 3T3)

The fibroblast cell line (NIH 3T3) culture has been seeded on the substrates at a density of 1.0×10^4 cells in a 96-well plate and incubated for 72 h at 37^0C in a CO_2 incubator. Ten µl of MTT (5mg/ml Phosphate buffered saline) is added to the wells, 4 h prior to the completion of incubation time. The plate is centrifuged at 1200×g for 10 min and 100 µl of DMSO is added after removing the supernatant, to dissolve the formazan formed. The absorbance is read at 530 nm after 5 min, in a microplate reader.

Haemolysis test

The haemolysis test has been carried out to investigate the haemocompatibility of the NCD samples and the uncoated silicon samples. Samples are taken in test tubes containing N-saline (0.9% NaCl) and incubated at 37 °C for 30 min for providing temperature stabilization. 0.2 ml of anticoagulated and diluted blood (N-saline: blood; 8: 10) is then added to the test tube, mixed properly and incubated for 60 min. The optical density (OD) of the incubated solution is measured in an UV spectrometer at 545 nm. Sodium carbonate (1%) has been used as a positive control and N-saline as a negative control. The haemolysis percentage is calculated using the formula [**1**, **20**].

$$\text{Haemolysis (\%)} = \frac{OD_{(\text{Uncd sample})} - OD_{(\text{negative})}}{OD_{(\text{positive})} - OD_{(\text{negative})}} \times 100$$

The accepted norm is that if the haemolysis percentage is less than 10 the test sample can be considered as haemocompatible and if it is less than 5 the material is highly haemocompatible.

Table 2. Composition of simulated body fluid (250 ml).

S. No.	Name of chemical	Quantity
1.	NaCl	3.27 gm
2.	$NaHCO_3$	1.13 gm
3.	KCl	0.18 gm
4.	$Na_2HPO_4.2H_2O$	0.089 gm
5.	MgCl2.6H2O	0.15 gm
6.	37 wt.% HCl	5 ml
7.	$CaCl_2$	0.139 gm
8.	$NaSO_4$	0.035 gm
9.	Tris buffer	3.27 gm

Simulated body fluid (SBF) adsorption assay

To know the effect of interaction of SBF on the NCD coated and uncoated silicon samples, SBF adsorption assay

has been performed in the similar way as given in references 1 and 21. The samples are soaked in the SBF solution under sterile conditions (using laminar flow) and kept for 30 days at room temperature.

Samples are taken out from SBF solution after 30 days and cleaned with deionized water for 2 minutes to remove the SBF solution which remains on the surface of the samples in liquid form. Prior and after the soaking in SBF, samples are analyzed by AFM to observe the changes in surface morphology. The ratio of the surface volume to the surface area of specimen is kept at 0.1 ml/mm^2. The composition of the simulated body fluid is given in **Table 2** [**1**, **13**]. All the constituents (NaCl, $NaHCO_3$, KCl, $K_2HPO_4.3H_2O$, $MgCl_2.6H_2O$, $CaCl_2$ and Na_2SO_4) are dissolved into 200 ml deionized water by continuous magnetic stirring at 37 °C and buffered at pH 7.4 with tris (hydroxymethyl) amminomethane ($(CH_2OH)_3CNH_3$) and hydrochloric acid (HCl). Finally, the volume is made up to 250 ml and the solution is filtered using 0.22 µm vacuum filter and stored at 4 °C until use.

Results and discussion

The Raman spectroscopy is the most reliable tool to confirm the formation of NCD films. Raman spectra of NCD films which are dominated by the G peak and D peak, can provide a view of sp^3 and sp^2 bonded carbon content at the grain boundaries by analyzing both G peak position and I(D)/ I(G). The Raman spectra of the NCD films are shown in **Fig. 1**. Four broad peaks have been observed in each spectrum. Peak centered at 1550 cm^{-1} (G peak) is due to sp^2 bonded graphite, the peak centered at 1345 cm^{-1} (D peak) is due to disorder in graphite [**22**, **23**].

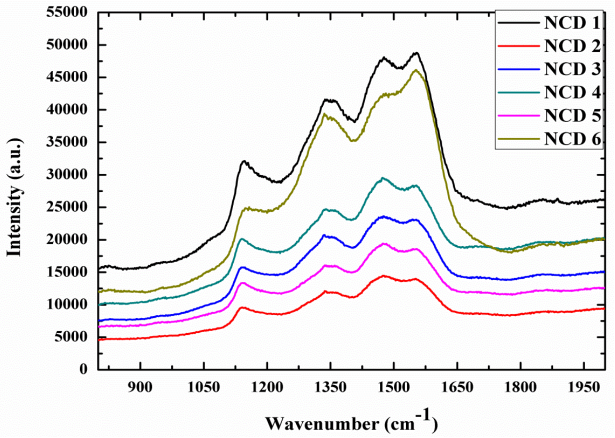

Fig. 1. Raman spectra of NCD samples.

Peaks centered at 1140 cm^{-1} and 1470 cm^{-1}, the typical Raman feature of NCD films, are associated with ν_1 and ν_3 vibration modes of transpolyacetylene co-deposited with diamond phase at the grain boundaries [**24-26**]. A small sharp peak around 1332 cm^{-1}, situated at right side of the D peak, represents diamond [**22**, **27**]. Raman spectra of NCD films differ drastically from that of single crystal diamond. The diamond peak at 1332 cm^{-1}is reduced strongly and the spectra are dominated by D and G peaks generated by sp^2 bonded carbon situated at the grain boundaries of the NCD films. The unusually high temperature stability of transpolyacetylene can be explained only if it is co-deposited with diamond phase [**28**, **29**].

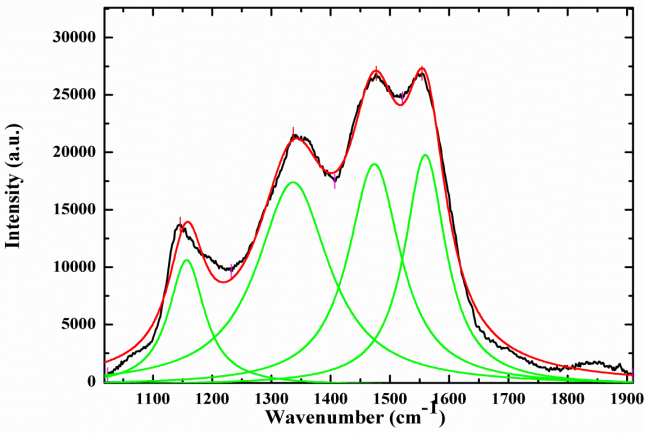

Fig. 2. De-convoluted Raman spectrum of NCD 1 sample.

The analysis of Raman spectra has been carried out by fitting using Lorentzian function after base line correction. The de-convoluted Raman spectrum of NCD 1 is shown in **Fig. 2.**

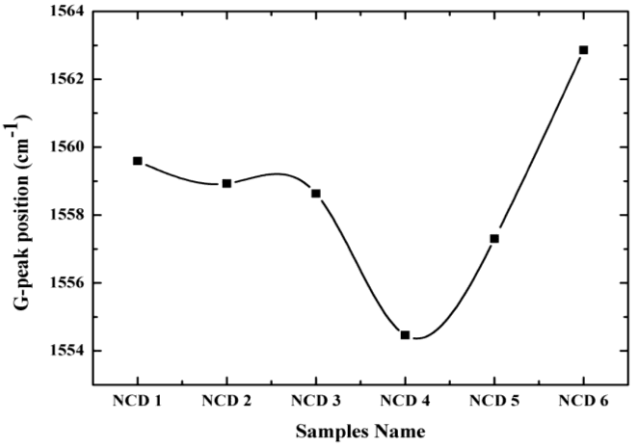

Fig. 3. Plot of G peak position for different NCD samples.

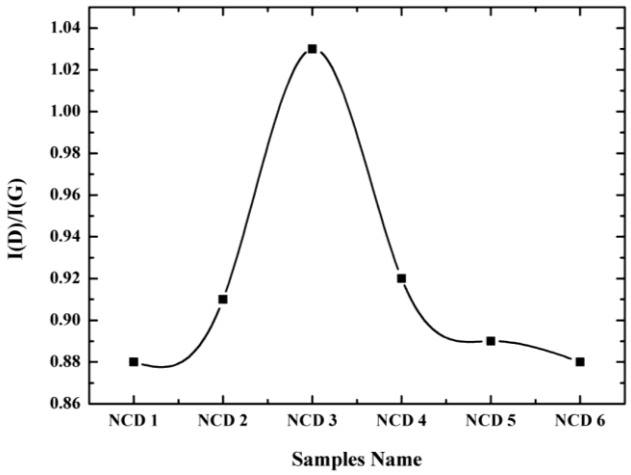

Fig. 4. Plot of I(D)/I(G) ratio for different NCD samples.

The G peak position and I(D)/I(G) ratio are calculated from these fittings and plotted for different samples **(Figs. 3 and 4).** The G peak positions first decreases and after reaching minimum it increases **(Fig. 3)**. It has also been observed that the I(D)/I(G) ratio first increases and after reaching maximum it decreases **(Fig. 4)**. Three stage model

of Robertson and Ferrari [**4**, **22**] has been used for the analysis of variation in G peak position and I(D)/I(G) ratio. Very slight change in the G peak position has been observed for NCD 1, NCD 2 and NCD 3, which correspond to 800, 1000 and 1200-watt microwave power, respectively. However, there is sharp increase in I(D)/I(G) ratio, indicates the increase in nanocrystalline graphite at the boundaries. For samples NCD 4, NCD 5 and NCD 6 which correspond to 1400, 1600 and 1800-watt microwave power, respectively, the G peak position increases rapidly and I(D)/I(G) ratio decreases indicating an increase in sp^3 bonded carbon.

Hence, it can be concluded that with the increase of microwave power (up to 1200 watt) initially formation of nanocrystalline graphite takes place and further increase in microwave power promotes the formation of sp^3 bonded carbon at the grain boundaries. It can also be concluded that at low microwave power grain boundaries contain more sp^2 bonded carbon compared to the films deposited at high microwave power. It can also be argued that the films with high sp^3 content at the grain boundaries will also have sharp grain boundaries.

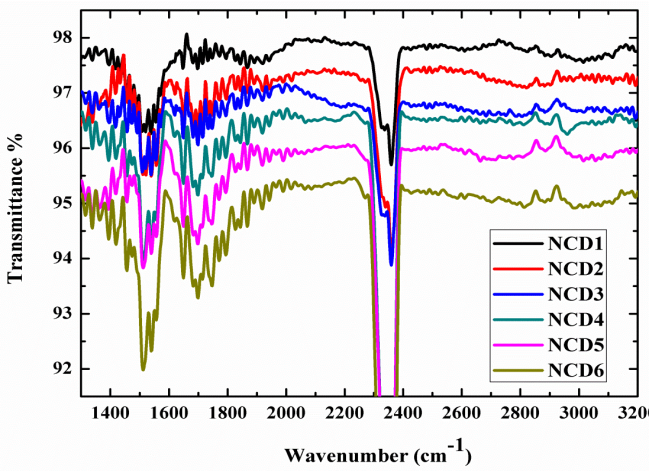

Fig. 5. FTIR spectra of NCD samples.

FTIR is the widely used technique to characterize the bonding and chemical bondings present in the material. FTIR spectra of NCD films are shown in **Fig. 5**. Peaks below 2000 cm^{-1} are because of C-C bending mode. Strong peak centered around 2350 $cm^{-1}$is because of CO_2.Peaks within 2800 – 3300 cm^{-1} are due to C-H stretching modes which confirm the presence of hydrogen at the grain boundaries of the films [**4**]. In NCD films the concentration of hydrogen is very small, however, its presence may affect the properties. It is difficult to quantify the amount of hydrogen in the films, however, it can be argued that the films with broad grain boundaries contain higher amount of hydrogen compare to the films having sharp grain boundaries.

Thickness of the samples has been measured using SEM by taking cross sectional image. SEM image of NCD3sample is shown in **Fig. 6**. Observed thickness of NCD1, NCD2, NCD3, NCD4, NCD5 and NCD6 are 4.38 µm, 8.63 µm, 7.11 µm, 4.06 µm, 4.57 µm and 3.83 µm, respectively. It has been reported that the thickness of the films depends on microwave power and C_2 emission intensity [**30**]. It has been observed that the protective coating of the order of 500 nm or less is sufficient to prevent the interaction of SBF with substrate surface [**1**]. In present investigation, significant thick films (more than 1 µm) have been deposited which is suitable for protective coating for bio devices.

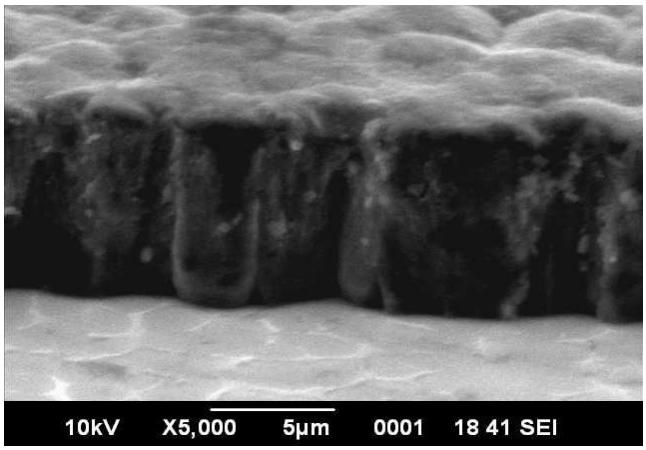

Fig. 6. SEM image of cross-section of NCD 3 sample.

Good hydrophobic property is desirable for a bio-material. Hydrophobic surface will provide poor adhesion to body fluid, blood and cells with the surface of implants which minimize the infection, toxicity, thinning, cell death etc. Hydrophobicity of the samples has been measured by using optical contact angle setup. Optical contact angle of deposited NCD films are shown in **Fig. 7**. The results infer that all the deposited NCD films have contact angle greater than 90^0 which shows that all NCD films are hydrophobic in nature **(Fig. 7)**. It has been observed that the contact angles show an increasing tendency with microwave power, used for the deposition of NCD films.

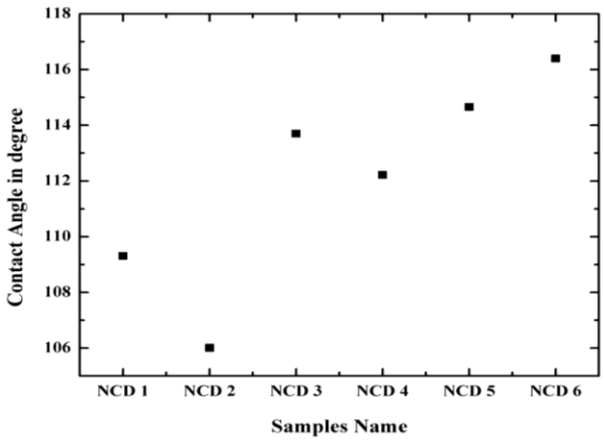

Fig. 7. Contact angles of NCD samples.

Lymphocytes play an important role in responding against any foreign material inside the body and Fibroblasts play a particular role in the wound repair process as one of the first tissues involved in repair of damaged tissue. Device implanted inside the body come in direct contact with Lymphocytes and Fibroblast. Surface properties of implanted device can influence cellular processes of attachment, spreading and growth, which influence the degree of conformational changes of the adsorbed proteins and polysaccharide of the cell and then affect the cell

growth. Effect of NCD coated Si substrates on lymphocytes viability is shown in **Fig. 8**. The significant loss in the cell viability has been observed in the presence of uncoated silicon substrates at 72h (~ 60% cells remained viable). However, the NCD coating on Si has increased the viability of the cells. Cell viability of lymphocytes cultured on NCD coated substrate is more than 90 %.

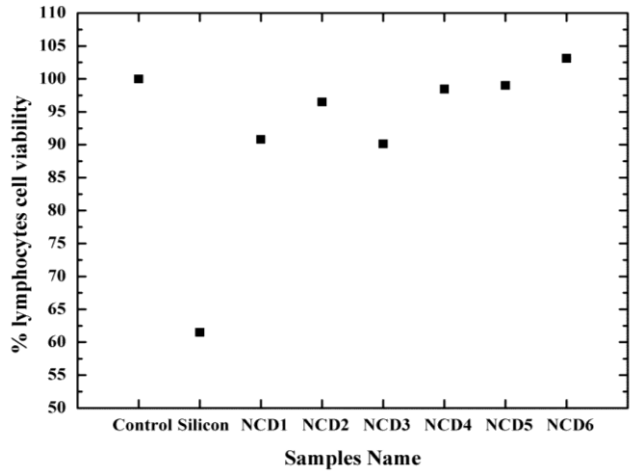

Fig. 8. Percentage cell viability of lymphocytes on uncoated and NCD coated silicon samples.

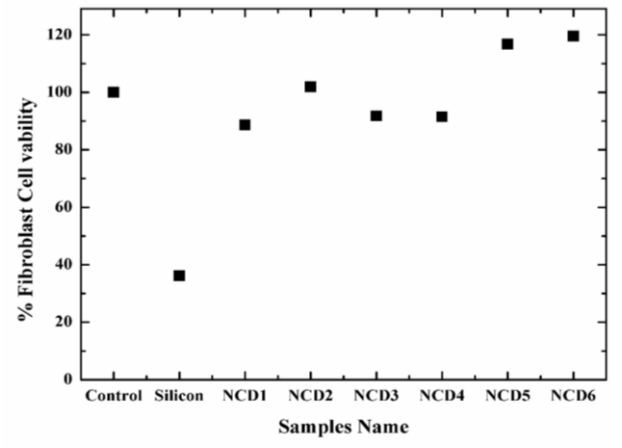

Fig. 9. Percentage cell viability of fibroblast cell line on uncoated and NCD coated silicon samples.

This indicates that there is no significant loss in cell viability as compared to control. For few samples it is more than 100%. One sample (NCD 6), showing the cell viability more than control, indicates that NCD also promotes the cell growth. Hence, NCD may be a better substrate for lymphocytes cell growth. It has also been observed that the cell viability increases with microwave power.

Fig. 9 shows the cell viability of Fibroblast cells cultured on uncoated and NCD coated samples. It has been observed that the NCD coating has reduced the Si induced loss in cell viability in Fibroblast cell line. In the presence of Si, only 35% cells remained viable while ~ 90 % cells are viable when cultured on the NCD coated samples. In conclusion, there is no significant loss in the fibroblast cells viability in presence of NCD coating. Highest cell growth has been observed for the films deposited at high microwave power (NCD 5 and NCD 6). For these films, the viability is more than control **(Fig.9)**.

Haemolysis test has been carried out to access the compatibility of the NCD coated silicon substrate with blood. The results of the haemolysis test are shown in **Fig. 10**. The haemolysis percentage of uncoated Si is ~ 20% and for NCD coated Si, it is less than 10. The uncoated Si is found to be uncompatible (as haemolysis % >> 10) in blood, whereas all NCD coated Si samples are found to be highly haemocompatible **(Fig.10)**. Percentage haemolysis decreases as the microwave power used for the deposition of NCD films increases.

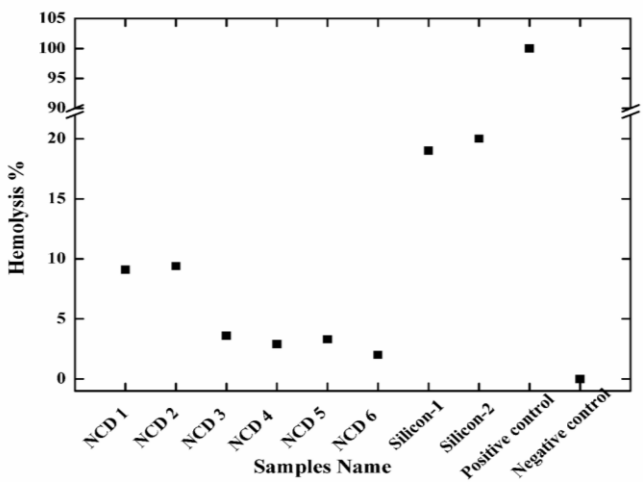

Fig. 10. Percentage haemolysis of uncoated and NCD coated silicon samples.

Observed results can be understood with the help of Raman spectra. The structure of the NCD films consists of nano diamonds separated by the grain boundaries. The grain boundaries of NCD films are complex and have sp^3, sp^2, sp^{2+x} and hydrogen. Raman spectra shows that films deposited at low microwave power have relatively broader grain boundaries which may contain high hydrogen content, sp^2 and other sp^{2+x} bonded carbon species compared to the films deposited at high microwave power. Grain boundaries of the films deposited at high microwave power have high sp^3 bonded carbon. Presence of hydrogen and sp^{2+x} bonded carbon in the grain boundaries play a crucial role to determine the biocompatible behavior of the NCD films. Experimental observations show that percentage of cell viability of Lymphocytes and Fibroblast cells increases with microwave power used for the deposition of NCD films. It can be argued that effect on the cell viability due to the interaction of diamond will be the same for all the films. Hence, the change in the cell viability is because of the sp^{2+x}, hydrogen and other unstable species present at the grain boundaries. The decrease in cell viability is because of the interaction of the cells with these species. Interaction may cause of the release of hydrogen from grain boundaries and reaction with the unstable carbon species. NCD samples with high sp^3 concentration, which results the sharp grain boundaries and hence low hydrogen and other unstable species at the grain boundaries, show better cell viability. Silicon surface which is considered to be more susceptible to hydrogen compared to the diamond show poor cell viability. Results of contact angle and haemolysis can also be understood with the help of Raman spectra.

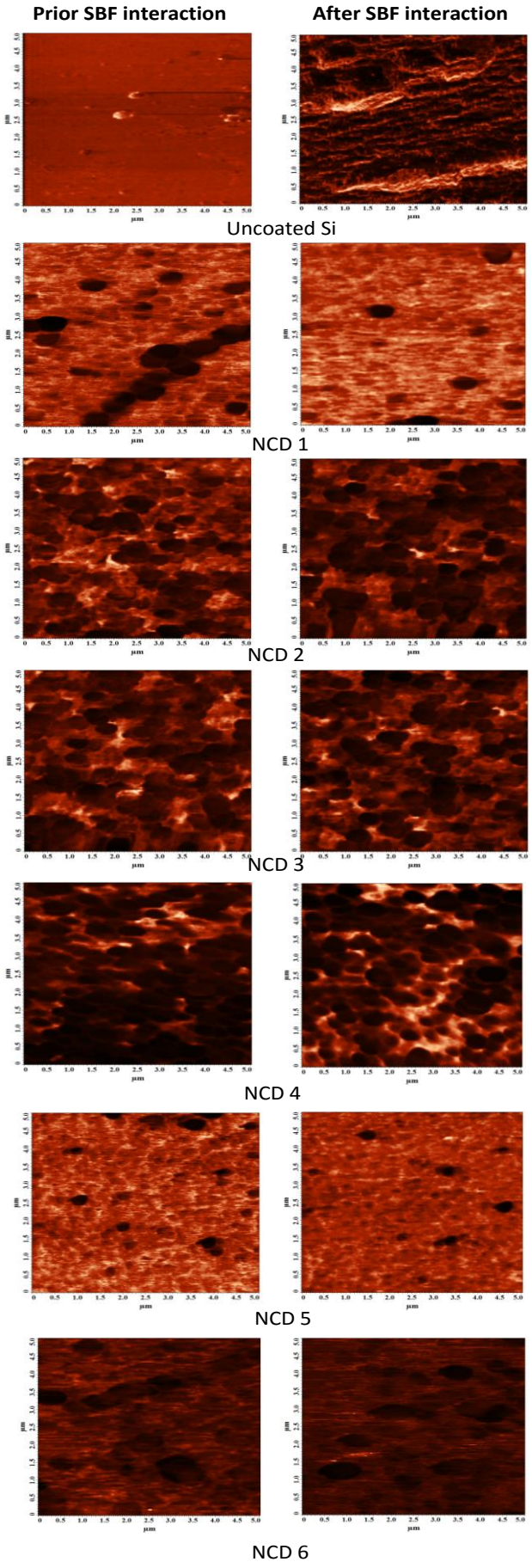

Fig. 11. AFM images of uncoated and NCD coated silicon samples before and after interaction with SBF.

High contact angle has been observed for the samples containing high sp^3 content. Similarly, percentage haemolysis is low for the samples having high sp^3 content at the boundaries. Simulated body fluid adsorption assay has been carried out by the AFM images of the samples before and after interaction with SBF. Images are shown in **Fig.11**. Effect of interaction of SBF on Si surface has been clearly observed. However, Si itself is considered as an inert surface but the longtime interaction with body fluid starts its degradation [1], while NCD coated Si surfaces have very less changes in their surface morphologies. The bio-compatibility of NCD samples mainly depends on the behaviour of the grain boundaries. Diamond part of the NCD films can be considered as inert which will behave similar to the bulk diamond. It is the grain boundaries which contain complex structure that may be affected by SBF [1]. The width of the grain boundaries in NCD films is of the order of nanometer, hence, very small change or no change on the surface has been observed after interaction with SBF in the present investigation.

Conclusion

The present study shows that NCD films have strong potential to replace the existing biocompatible coatings. Hydrophobicity, cell viability of lymphocytes and fibroblast cells, haemocompatibility, and SBF assay are carried out to analyse the biocompatible behaviour of the NCD films. Raman spectra confirm the formation of NCD films. Presence of hydrogen, which is present at the grain boundaries, has been confirmed by FTIR spectra. SEM image imply the deposition of significant thick films suitable for protective coatings. Optical contact angle analysis demonstrates the hydrophobic nature of NCD films. The cell viability of lymphocytes and fibroblast cell lines cultured on NCD films has been investigated by MTT assay. There is a significant loss in the cell viability of both the cell types cultured on Si substrate. NCD coating has reduced the loss in cell viability significantly. Few samples, showing the cell viability more than control, indicate that NCD may promote the cell growth. The seeded films allow reproduction of the typical features of the two cell populations, further suggesting the lack of cytotoxicity of this coating. Different percentage in cell viability of different NCD samples has been explained using analysis of Raman Spectra. The change in the cell viability is because of the interaction of the cells with sp^{2+x}, hydrogen and other unstable species present at the grain boundaries. Sharp grain boundaries because of the high sp^3 concentration result low probability of reaction of hydrogen and other unstable species with the cells, hence, show better cell viability. It has been found that NCD coated surface also show good protection against SBF. The haemolysis test with blood shows that uncoated silicon substrate is not hemocompatible and the NCD films are highly haemocompatible. Thus, the cellular biocompatibility of the NCD coatings, allied with the excellent physicochemical performance, anticipates a wide range of applications in the biomedical field. NCD can provide an outstanding platform material for a new generation of advanced implantable biomedical devices.

Acknowledgements
The authors are thankful to Dr. S. Khandelwal, Immunotoxicology lab., IITR, Lucknow, for her support and guidance for Lymphocyte and

fibroblast cell line culture assay. The authors are also thankful to DST-FIST for Raman spectrometer.

References

1. Sharma, R.; Pandey, A.K.; Sharma, N.; Sasmal, D.; Barhai, P.K.; *Surf coat Technol.* **2010**,*205*,2495. **DOI:** 10.1016/j.surfcoat.2010.09.054.
2. Von, E.C.; Jansen, B.; Kohnen, W.; Becker, K.; *Drugs*. **2005**, *65*, 179. **DOI:** 10.2165/00003495-200565020-00003
3. Pierson, O.H.; Handbook of Carbon, Graphite, Diamond and Fullerenes Properties, Processing and Applications; Noyes Publications; Park Ridge, New Jersey: U.S.A **1993**.
4. Robertson, J.; *Mater. Sci. Eng. R.* **2002**, *37*, 129. **DOI:** 10.1016/S0927-796X(02)00005-0
5. Gruen, D.M.; *Annu. Rev. Mater. Sci.* **1999**, *29*, 211. **DOI:** 10.1146/annurev.matsci.29.1.211
6. Ullah, M.; Ahmed, E.; Elhissi, A.; Ahmed, W.; *Bull. Mater. Sci.* **2014**, *37*, 579. **DOI:** 10.1007/s12034-014-0669-y.
7. Lin, Z.; Lv, S.B.; Yu, Z.J.; Li, M.; Lin, T.Y.; Ba, D.C.; Choi, C.K.; Lee, I.S.; *Surf. Coat. Technol.* **2008**, *202*, 5386. **DOI:** 10.1016/j.surfcoat.2008.06.071.
8. Ohgoe, Y.; Hirakuri, K.K.; Tsuchimoto, K.; Friedbacher, G.; Miyashita, O.; *Surf. Coat. Technol.* **2004**, *184*, 263. **DOI:** 10.1016/j.surfcoat.2003.10.009.
9. Matsumoto, R.; Sato, K.; Ozeki, K.; Hirakuri, K.; Fukui, Y.; *Diamond Relat. Mater*. **2008**, *17*, 1680. **DOI:** 10.1016/j.diamond.2008.02.027.
10. Li, D.J.; Cui, F.Z.; Gu, H.Q.; Li, W.Z.; *Vacuum* **2000**,*56*, 205. **DOI:** 10.1016/S0042-207X(99)00183-9.
11. Li, D.J.; Cui, F.Z.; Gu, H.Q.; *Appl. Surf. Sci.* **1999**, *137*, 30. **DOI:** 10.1016/S0169-4332(98)00485-1.
12. Thomson, L.A.; Law, F.C.; Rushton, N.; Franks, J.; *Biomaterials* **1991**, *12*, 37. **DOI:** 10.1016/0142-9612(91)90129-X
13. Salgueiredo, E.; Vila, M.; Silva, M.A.; Lopes, M.A.; Santos, J.D.; Costa, F.M.; Silva, R.F.; Gomes, P.S.; Fernandes, M.H.; *Diamond Relat. Mater*. **2008**, *17*, 878. **DOI:** 10.1016/j.diamond.2007.08.019.
14. Kumar, S.; Sarangi, D.; Dixit, P.N.; Panwar, O.S.; Bhattacharyya, R.; *Thin Solid Films* **1999**, *346*, 130. **DOI:** 10.1016/S0040-6090(98)01500-4
15. Qiang, L.; Zhang, B.; Zhou, Y.; Zhang, J.; *Solid State Sci*. **2013**, *20*, 17. **DOI:** 10.1016/j.solidstatesciences.2013.03.003
16. Amaral, M.; Gomes, P.S.; Lopes, M.A.; Santos, J.D.; Silva, R.F.; Fernandes, M.H. J.; *Nanomatt.* **2008**, 1. **DOI:** 10.1155/2008/894352
17. Amaral, M.; Dias, A.G.; Gomes, P.S.; Lopes, M.A.; Silva, R.F.; Santos, J.D.; Fernandes, M.H. J.; *Biomedical Matt. Res. Part A*, **2008**, 91. **DOI:** 10.1002/jbm.a.31742
18. Kumar, A.; Sasmal, D.; Bhaskar, A.; Mukhopadhyay, K.; Thakur, A.; Sharma, N.; *Environ. Toxicol*. **2014**. **DOI:** 10.1002/tox.22091
19. Mosmann, M.; *J. Immunol. Meth.* **1983**, *65*, 55. **DOI:** 10.1016/0022-1759(83)90303-4
20. Chowdhury, S.K.R.; Mishra, A.; Pradhan, B.; Saha, D.; *Wear* **2004**, *256*, 1026. **DOI:** 10.1016/S0043-1648(03)00535-0.
21. Tas, A.C.; *Biomaterials*, **2000**, *21*, 1429. **DOI:** 10.1016/S0142-9612(00)00019-3
22. Ferrari, A.C.; Robertson, J.; *Phys. Rev. B* **2000**, *61*, 14095. **DOI:** 10.1103/PhysRevB.61.14095
23. Tuinstra, F., Koenig, J.L.J.; *Chem. Phys.* **1970**, *53*, 1126. **DOI:** org/10.1063/1.1674108
24. Nemanich, R.J.; Glass. J.T.; Lucovsky, G.; Shroder, R.E. *J. Vac. Sci. Technol.* **1988**, *A6*, 1783. **DOI:** 10.1116/1.575297
25. Piazza, F.; Golanski, A.; Schulze, S.; Relihan, G.; *Appl. Phys. Lett.* **2003**, *82*, 358. **DOI:** 10.1063/1.1538349.
26. Yacoby, Y.; Roth, S.; *Solid State Comm.* **1985**, *56*, 319. **DOI:** 10.1016/0038-1098(85)90393-X.
27. Knight, D.S.; White, W.B.J.; *Mater. Res.* **1989**, *4*, 385. **DOI:** 10.1557/JMR.1989.0385.
28. Klauser, F.; Steinmu¨ller Nethl, D.; Kaindl, R.; Bertel, E.; Memmel, N.; *Chem. Vap. Deposition* **2010**, *16*,127. **DOI:** 10.1002/cvde.200906827.
29. Pez-Rı´os, T.L.; Sandre, E.; Leclerque, S.; Sauvain, E.; *Phys. Rev. Lett*. **1996**, *76*, 4935. **DOI:** 10.1103/PhysRevLett.76.4935.
30. Sharma, R.; Woehrl, N.; Vrućinić, M.; Timpner, M.; Buck, V.; Barhai, P.K.; *Thin Solid Films* **2011**, *519*, 7632. **DOI:** 10.1016/j.tsf.2011.05.006.

